Proc. Natl. Acad. Sci. USA
Vol. 87, pp. 8145–8149, October 1990
Neurobiology

When is an inhibitory synapse effective?

(shunting inhibition/cable model/electrodiffusion model/dendritic spines)

NING QIAN*† AND TERRENCE J. SEJNOWSKI*‡

*Computational Neurobiology Laboratory, Salk Institute, 10010 North Torrey Pines Road, La Jolla, CA 92037; †Department of Biophysics, The Johns Hopkins University, Baltimore, MD 21218; and ‡Department of Biology, University of California, San Diego, La Jolla, CA 92037

Communicated by F. H. C. Crick, July 24, 1990 (received for review January 9, 1990)

ABSTRACT **Interactions between excitatory and inhibitory synaptic inputs on dendrites determine the level of activity in neurons. Models based on the cable equation predict that silent shunting inhibition can strongly veto the effect of an excitatory input. The cable model assumes that ionic concentrations do not change during the electrical activity, which may not be a valid assumption, especially for small structures such as dendritic spines. We present here an analysis and computer simulations to show that for large Cl^- conductance changes, the more general Nernst–Planck electrodiffusion model predicts that shunting inhibition on spines should be much less effective than that predicted by the cable model. This is a consequence of the large changes in the intracellular ionic concentration of Cl^- that can occur in small structures, which would alter the reversal potential and reduce the driving force for Cl^-. Shunting inhibition should therefore not be effective on spines, but it could be significantly more effective on the dendritic shaft at the base of the spine. In contrast to shunting inhibition, hyperpolarizing synaptic inhibition mediated by K^+ currents can be very effective in reducing the excitatory synaptic potentials on the same spine if the excitatory conductance change is less than 10 nS. We predict that if the inhibitory synapses found on cortical spines are to be effective, then they should be mediated by K^+ through $GABA_B$ receptors.**

Shunting inhibition occurs when the reversal potential of the synapse is approximately equal to the resting membrane potential. This occurs when the inhibitory current is carried by Cl^- ions or by a particular combination of K^+ and Na^+ or Ca^{2+} ions. This type of inhibitory input is silent: it does not change the membrane potential directly, but it can reduce the depolarization caused by excitatory synaptic inputs (1, 2). A measure of the effectiveness of such shunting inhibition is the ratio of the maximum depolarization at a reference point in the neuron caused by an excitatory input alone to the depolarization when both the excitatory and the inhibitory inputs are present. This ratio, called the F factor (2), is equal to 1 if the inhibition has no effect on the excitation. One obvious requirement for effective inhibition is that its time course should overlap substantially with the excitatory synaptic conductance change.

Cable Model Predictions

When does the cable model predict that inhibition is effective? Consider first the case in which the excitatory and inhibitory synapses are very close to each other. According to the cable model, the excitatory and the inhibitory synaptic currents are, respectively, given by

$$I_e(t) = G_e(t)[V(t) - E_e], \qquad [1]$$

and

$$I_i(t) = G_i(t)[V(t) - E_i] \approx G_i(t)[V(t) - V_{rest}], \qquad [2]$$

where E_e and E_i are the reversal potentials of the excitatory and the inhibitory synapses, G_e and G_i are the transient synaptic conductances, V is membrane potential at the synapse, and V_{rest} is the resting membrane potential (3).

We have assumed in Eq. **2** that the reversal potential for shunting inhibition is very close to the resting membrane potential. In contrast, the excitatory inputs usually cause conductance increases to ions such as Na^+ or Ca^{2+} that have a reversal potential, E_e, well above resting membrane potential. The inhibition will be effective if $|I_i|$ is comparable to $|I_e|$. This requires, first, that G_i be larger than G_e. Second, V should be well above the resting membrane potential so that the driving force for the inhibition ($V - V_{rest}$) is comparable to the driving force for the excitation ($V - E_e$). This in turn requires that G_e be large and/or that the synapses are on small structures, such as spines or thin dendrites, where input resistances are large and small synaptic conductance change can cause a large depolarization. (Large inhibitory driving forces can also be achieved when the cell is firing an action potential; see *Discussion*.) In summary, for shunting inhibition to be effective when excitation and inhibition are located close to each other, the cable model requires that the synapses should be on small structures and $G_i > G_e >> G_{rest}$, where G_{rest} is resting conductance of the membrane at the synapse. For stationary synaptic inputs, an explicit expression for the F factor can be derived (2, 4).

In their analysis and simulations of shunting inhibition, Koch *et al.* (2) mainly considered large synaptic conductances on spines and distal (thin) dendrites that satisfy the inequalities discussed above. Their G_e was as large as 10 nS and G_i was 100 nS, but more recent physiological data suggest that G_e should be ≈1 nS (5, 6). They also found that, for large excitatory conductances, inhibition on the direct path to the cell body was also effective, and that the most effective location for the inhibition moves toward the soma as the excitatory conductance increases (4). Two opposing factors explain the phenomenon: when the inhibition is on the direct path from excitation to the soma, I_i is smaller because, at the site of inhibition, the membrane is less depolarized; but I_e is also smaller because, at the site of excitation, the membrane is more depolarized. They also found that when the inhibition was more distal than the excitatory synapse, the inhibition was no longer effective. In this case, the resistance from the excitatory synapse to the cell body is much less than the resistance to the inhibitory synapse at the distal tip, so less current is shunted. Finally, Koch *et al.* (2) mentioned that increasing the value of the cytoplasmic resistivity and the membrane resistance increased the effectiveness of inhibition. This occurred because the membrane depolarization was larger, which made the driving force for the inhibitory

The publication costs of this article were defrayed in part by page charge payment. This article must therefore be hereby marked "*advertisement*" in accordance with 18 U.S.C. §1734 solely to indicate this fact.

Abbreviation: GABA, γ-aminobutyric acid.

current larger and the driving force for the excitatory current smaller.

The cable model fails for small structure and large conductance changes (7, 8), precisely the conditions required for effective shunting inhibition by the cable model. Briefly, the cable model assumes (*i*) that the membrane Nernst potentials are constant, (*ii*) that the longitudinal resistivities for all the ions are constant and can be combined into a single parameter, and (*iii*) that the longitudinal diffusion of ions can be neglected. These assumptions are invalid when there is a large spatial and/or temporal intracellular ionic concentration gradient. We have developed an electrodiffusion model for dendrites and spines that should give more accurate predictions under these circumstances (8).

Electrodiffusion Model Predictions

The electrodiffusion model predicts that the shunting inhibition cannot be effective on small structures for the following reasons. Consider first the case in which the conductance changes are large. If the inhibitory current is carried by Cl^- ions, then during a large conductance change the Cl^- concentration in a small structure such as a spine or a thin dendrite will very rapidly increase. The Nernst potential for Cl^- becomes more positive and the inhibition is ineffective. Changes in the Cl^- Nernst potential have been reported (9, 10). If the conductance changes are small, then the concentration changes for Cl^- are small and the electrodiffusion model will reduce to the cable model. Thus, shunting inhibition will not be effective because the membrane depolarization is small and the driving force for the inhibitory current is much smaller than that for the excitatory current, as discussed in the previous section. As a consequence, the electrodiffusion model predicts that the shunting inhibition can never be very effective in small structures.

A similar analysis can be applied for hyperpolarizing inhibition carried by K^+. When both the excitatory and the inhibitory synaptic conductances are large on a small structure, K^+ hyperpolarizing inhibition is just as ineffective as the Cl^- shunting inhibition because of large ionic concentration changes. However, the situation for small synaptic conductances is different. The reversal potential for K^+ is sufficiently below the resting potential that the driving force for the inhibition can be large even at the resting potential. In addition, the intracellular K^+ concentration is much higher than Cl^- and therefore the percentage change is usually smaller. These statements will be made quantitatively precise in the numerical simulations presented below based on both the cable and the electrodiffusion models.

Simulations

The electrodiffusion model is based on the Nernst–Planck equation, which considers the longitudinal diffusion process as well as the driving force due to the potential gradient. We previously (8) showed that the veto effect of shunting inhibition was not significant on spines when the large conductance changes to Na^+ and K^+ used by Koch *et al.* (2) were applied to the electrodiffusion model. We extend these results to shunting inhibition, which was modeled by transient Cl^- conductance change. Excitation was modeled by a combination of transient conductance changes to Na^+ and K^+, with the K^+ conductance equal to one-tenth of Na^+ conductance (11). The synaptic reversal potential under this combination is ≈50 mV. We also made simulations with the reversal potential of the excitatory synapse equal to 0 mV and similar conclusions were obtained. Ionic driving forces similar to Eqs. **1** and **2** were used for the electrodiffusion model rather than the constant field approximation used in ref. 8. The Nernst potentials were updated at each time step according to the instantaneous ionic concentrations. We varied the magnitudes and durations of the conductance changes and the spine neck dimensions. We also compared the effectiveness of inhibition on the spine with inhibitory input on the dendrite at the base of the spine, as shown in Fig. 1. The standard parameters used and details of the simulations are summarized in the legend to Fig. 1; any variation will be explicitly mentioned.

Synapses on spines. Approximately 7% of the spines on pyramidal cells in visual cortex have both excitatory and inhibitory profiles (12). It has been suggested that this type of

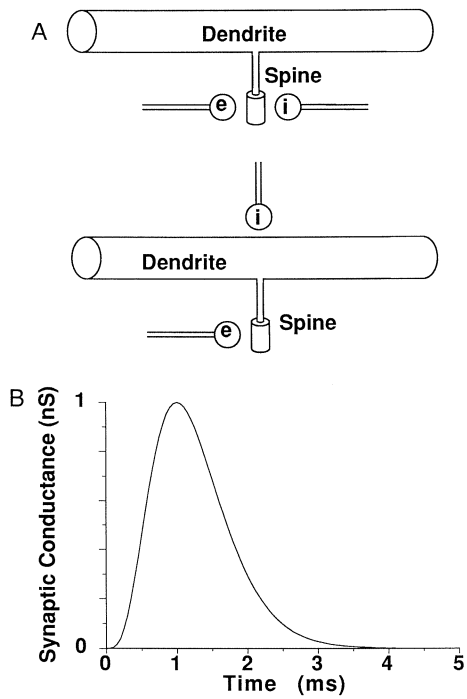

FIG. 1. (*A*) Geometry of the dendrite and spine for the simulations showing excitation and inhibition on the spine head (*Upper*) and inhibition on the dendritic shaft at the base of the spine (*Lower*). The spine was located in the center of a dendrite with a total length of 300 μm and a diameter of 1 μm; the spine neck was 1 μm long and 0.1 μm in diameter; the spine head was 0.69 μm long and 0.3 μm in diameter. In the simulations of the electrodiffusion model, sample points in the dendrite were 10 μm apart and the integration time step was 0.1 μs; in the spine head and neck the spacing was 0.173 μm and 0.167 μm, respectively, and the time steps were 2 ns. The model had a total of 41 sample points: 31 in the dendrite, 6 in the spine neck, and 4 in the spine head. In the conventional cable model, only 33 lumped compartments were used (1 for head, 1 for neck, and 31 for dendrite) because of the large space constant. The time step for spine head and neck was 0.1 μs and that for the dendrite was 1 μs. (*B*) Excitatory and inhibitory synaptic conductance changes were modeled by $G(t) = G_M(et/t_{peak})^4 e^{-4t/t_{peak}}$, where t_{peak} is the time to reach the peak conductance, G_M. A graph of this expression is shown with t_{peak} = 1 ms, and G_M = 1 nS. Parameters used in our simulations were as follows: t_{peak} = 1 ms; membrane capacitance C_m = 1 $\mu F/cm^2$; diffusion coefficients $D_K = 1.96 \times 10^{-5}$ cm^2/s, $D_{Na} = 1.33 \times 10^{-5}$ cm^2/s, and $D_{Cl} = 2.03 \times 10^{-5}$ cm^2/s; resting membrane conductances of unit area $g_{K,rest} = 1.95 \times 10^{-4}$ S·cm², $g_{Na,rest} = 1.63 \times 10^{-5}$ S·cm² and $g_{Cl,rest} = 3.89 \times 10^{-5}$ S·cm²; initial intracellular concentrations $n_{K,0}$ = 140 mM, $n_{Na,0}$ = 12 mM, and $n_{Cl,0}$ = 5.5 mM; extracellular concentrations $n_{K,out}$ = 4 mM, $n_{Na,out}$ = 145 mM, and $n_{Cl,out}$ = 120 mM. With this set of parameters, the resting membrane potential was −78 mV. The Nernst potentials for K^+, Na^+, and Cl^- were −90, 63, and −78 mV, respectively. Total membrane resistivity R_m was 4000 Ω·cm². Total cytoplasmic resistivity R_i at rest was calculated (8) to be 87 Ω·cm. Total surface area of the spine head was 0.65 μm². Some of these parameters were varied as explained in the relevant figures and tables. The sources for these parameters are given in ref. 8.

Table 1. F factors for Cl^- inhibition

	$G_{Na,M}$ = 0.1 nS		$G_{Na,M}$ = 1.0 nS		$G_{Na,M}$ = 10 nS	
$G_{Cl,M}/G_{Na,M}$	Diffusion	Cable	Diffusion	Cable	Diffusion	Cable
1	1.02	1.02	1.10	1.17	1.23	1.65
10	1.10	1.20	1.20	2.74	1.26	7.56
100	1.16	3.04	1.19	18.63	1.25	66.20
1000	1.14	20.35	1.19	163.86	1.25	602.19

F factors at the spine head when both excitatory and Cl^--mediated inhibitory synaptic inputs are located on the same spine predicted by both the electrodiffusion model and the cable model.

spine forms a "module for performing a selective AND-NOT-like operation effectively decoupled from other such subunits" (13). We modeled a spine located in the middle of a 300-μm-long dendrite and the response at the spine head was used to calculate F factors. Our simulation results based on both the cable model and the electrodiffusion model are shown in Table 1. The cable model indeed showed strong veto effects especially when the conductances were large, as predicted. However, our electrodiffusion model showed no significant veto effect over a wide range of conductances. Note also that when the $G_{Cl,M}/G_{Na,M}$ ratio was increased, there were cases in which the F factor decreased slightly. This occurred because the Cl^- Nernst potential shifted so much that it depolarized the membrane away from its resting level. A Cl^- conductance change alone, however, did not cause any depolarization because there was no driving force and therefore no concentration change.

The difference between the cable model and the electrodiffusion model decreased as the synaptic conductances decreased. For $G_{Na,M}$ = 0.1 nS, the two models were essentially identical and both predicted that the inhibition was ineffective. However, for longer durations of the synaptic input, the two models may not agree even for synaptic conductance changes as small as 0.1 nS (see *Discussion*). The details of the postsynaptic responses on the spine head are shown in Fig. 2.

Quantal analysis on excitatory postsynaptic potentials in area CA3 of the rat hippocampus (5, 6) gave a quantal conductance of $\approx$1 nS at mossy fiber synapses. Therefore, the synaptic conductance change due to a single presynaptic action potential should be a few nanosiemens. Similar measurements of unitary inhibitory conductance performed on CA3 pyramidal cells of guinea pig hippocampus obtained a value of 5–9 nS (14). However, the conductance of synapses on pyramidal cells in cerebral cortex may be much smaller. In the following simulations, we fixed $G_{Na,M}$ at 1 nS and varied $G_{Cl,M}$ unless otherwise indicated.

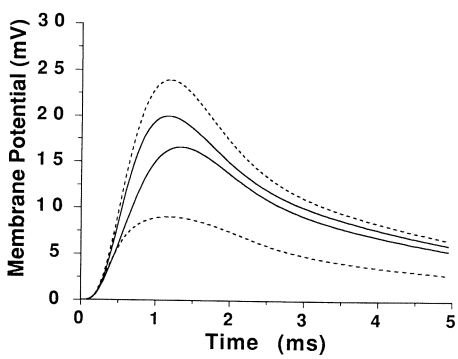

FIG. 2. Postsynaptic responses relative to the resting level at the spine head calculated with the electrodiffusion model (solid lines) and the cable model (dotted lines). Two traces are shown for each model: the top trace is the response with excitatory synaptic input alone and the bottom trace is the response to both excitatory and shunting inhibitory inputs. Excitatory synaptic input, $G_{Na,M}$ = 1 nS; inhibitory synaptic input, $G_{Cl,M}$ = 10 nS.

The morphologies of spines vary greatly. The critical parameters for our simulations were the diameter and length of spine neck, which were varied from 0.1 to 0.25 μm and from 0.4 to 1.0 μm, respectively, with the neck membrane area kept constant. We also considered the case in which there was no spine neck and the spine head was connected directly to dendrite. The cable model gave large F factors when the neck was long and narrow and/or $G_{Cl,M}$ was large, but the electrodiffusion model produced no F factor larger than 2 over the entire range. The effectiveness of inhibition was not very sensitive to the dimensions of the spine neck because of two competing effects that cancel: as the spine neck length was decreased and the diameter increased, the concentration changes in the spine were reduced, making the inhibition more effective. However, the input resistance of the spine head was also decreased, resulting in a smaller depolarization and a reduced driving force for the inhibition.

On-path inhibition. Inhibitory synapses on pyramidal neurons are commonly located on the dendritic shaft at the base of the spine (12, 15). The simulations in Fig. 3 show that dendritic on-path inhibition is much more effective than inhibition on the spine head. The ionic concentration changes were much smaller for the dendritic inhibition because the dendrite had a diameter of 1 μm, and hence the cable equation was a good approximation. Also, the driving force for the inhibition was strong because the spine was electrically coupled to the dendrite well enough that the excitation of the spine caused a large depolarization at the dendritic shaft.

Interactions between synapses on dendrites. We next studied interactions between excitatory and inhibitory synapses at adjacent sites on dendrites ranging in diameter from 0.1 to 2.0 μm. The predicted F factors for the cable model, given in Table 2, were very large when the dendritic diameter was small and the G_{Cl} was large. For the electrodiffusion model, two competing factors determined the effectiveness of inhibition: for dendrites with large diameters, the concen-

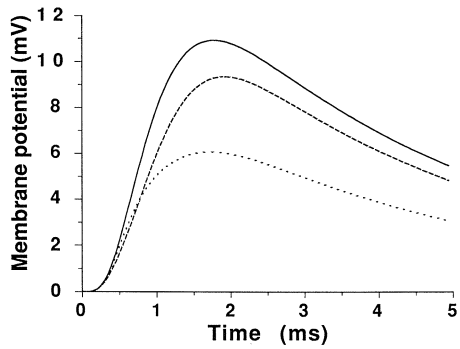

FIG. 3. Responses relative to the resting level at the dendritic shaft at the base of a spine under three conditions: no inhibition and the excitatory input ($G_{Na,M}$ = 1 nS) on the spine head alone (solid line), the excitatory input ($G_{Na,M}$ = 1 nS) and the inhibitory input ($G_{Cl,M}$ = 10 nS) both on the same spine head (dashed line), and the excitatory input ($G_{Na,M}$ = 1 nS) on the spine head and the inhibitory input ($G_{Cl,M}$ = 10 nS) on the dendritic shaft at the base of the spine (dotted line).

Table 2. F factors by electrodiffusion and cable models

	Dendritic diameter, μm				
$G_{Cl,M}/G_{Na,M}$	0.1	0.25	0.5	1.0	2.0
	Electrodiffusion				
0.1	1.07	1.04	1.02	1.01	1.00
1	1.47	1.45	1.18	1.07	1.03
10	1.87	1.66	2.26	1.66	1.31
100	1.91	2.67	3.43	3.10	3.25
	Cable				
0.1	1.08	1.06	1.04	1.02	1.01
1	1.72	1.39	1.19	1.08	1.04
10	8.31	5.16	3.03	1.88	1.38
100	73.07	43.15	22.46	11.01	5.65

F factors for both excitatory and inhibitory synapses on dendrites at the same site, with different dendritic diameters. $G_{Na,M}$ = 1 nS.

tration effects were small so the Nernst potential did not change very much and the inhibition was effective. However, the depolarization of the membrane from the resting level was smaller in larger dendrites, which made inhibition less effective. The F factors by electrodiffusion model (Table 2) were not monotonically increasing with increasing dendritic diameter because of these two factors and their interaction. For $G_i = G_e$ the first factor dominated and the inhibition was comparatively more effective on small dendrites. When $G_i \geq G_e$, the second factor dominated and the inhibition was more effective on large dendrites. In any case, when the dendritic diameter was 0.1 μm, the F factors were always <2, similar to the previous results for inhibition on spines.

K^+-mediated inhibition. The equilibrium potential for K^+ is generally below the resting membrane potential (12 mV below in our model) so that an increase in K^+ conductance leads to a hyperpolarization. In a previous study we found that inhibition on spines mediated by K^+ was not effective for excitatory conductances ≥10 nS (8). In this section, we consider excitatory conductances that are lower and more realistic for pyramidal neurons. We find that for smaller excitatory conductances, hyperpolarizing inhibition can be quite effective. Synaptic responses to $G_{Na,M}$ = 0.1 nS are shown in Fig. 4, which also shows that an inhibition of $G_{K,M}$ = 1 nS is very effective in reducing the response. In comparison, the inhibition due to a similar or much larger conductance change for Cl^- was not effective. For large excitatory conductance changes, the K^+ inhibition became as ineffective as Cl^- because of the large K^+ concentration changes that rapidly shift the K^+ Nernst potential, as shown in Table 3.

Inhibition mediated by K^+ in cortical neurons has a time course that can last for a significant fraction of a second when it is activated by $GABA_B$ receptors through guanine nucleotide-binding regulatory proteins (G proteins). We therefore studied the steady-state behavior following a step change in conductances of G_{Na} = 0.1 nS and G_K = 1 nS and found that the response at the spine head was ≈6.9 mV with excitation alone and 1.3 mV with both excitation and inhibition. In steady state, the K^+ efflux from the spine head was balanced by the K^+ diffusion from the dendritic shaft to the head.

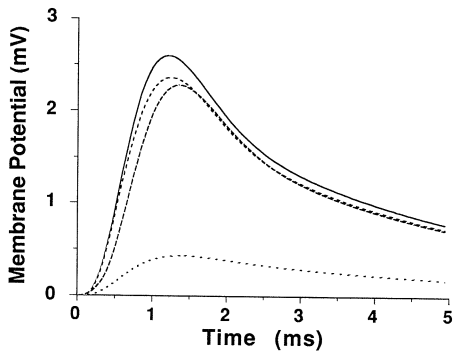

FIG. 4. Response relative to the resting level at the spine head to an excitatory input of $G_{Na,M}$ = 0.1 nS and one of the following three different inhibitory synaptic inputs: no inhibition (——), K^+ inhibitory synaptic input with $G_{K,M}$ = 1 nS (····), Cl^- inhibitory input with $G_{Cl,M}$ = 1 nS (- - -), and $G_{Cl,M}$ = 100 nS (–––).

Thus, the inhibition mediated by K^+ conductances remained effective for slow inhibitory synaptic potentials when the excitatory conductances were small. Since an excitatory synaptic conductance typically lasts for only a few milliseconds, an excitatory input arriving a few milliseconds earlier than the inhibitory input will not be affected by the inhibition. Once an inhibitory input is active, there is a long time window during which arriving excitatory inputs are inhibited.

Discussion

The major conclusion of this paper is that Cl^- shunting inhibition on spines cannot be effective regardless of how large the synaptic conductance changes are. Shunting inhibition is significantly more effective when it is on the dendritic shaft on path to the cell body. This may partly explain the anatomical findings that most synapses on spines are putatively excitatory and that the majority of the putative inhibitory synapses are found on dendritic shafts. For example, in hippocampal pyramidal cells, almost all synapses found on spines are excitatory (16). In the cat primary visual cortex only 7% of synapses on spines are inhibitory (12), although they comprise almost one-third of the total number of inhibitory synapses on a pyramidal cell. Shunting inhibitory synapses on spines may have other functions. Although they may not contribute significantly to the electrical responses of the cell, they can certainly cause large local ionic concentration changes that may be important in regulating certain cellular functions.

The inhibitory synapses on spines may contribute to the electrical responsiveness of a cell if they are mediated through K^+ currents. Our simulations predict that K^+ hyperpolarizing inhibition on a spine head can be very effective when the excitatory synaptic conductance changes are <10 nS. The major inhibitory neurotransmitter in the visual cortex is γ-aminobutyric acid (GABA); $GABA_A$ receptors are coupled to Cl^- channels and $GABA_B$ receptors are linked to K^+ channels. Therefore, we specifically predict that the inhibition on spines is mediated by the $GABA_B$ receptors. This

Table 3. F factors for K^+ inhibition

	$G_{Na,M}$ = 0.1 nS		$G_{Na,M}$ = 1.0 nS		$G_{Na,M}$ = 10 nS	
$G_{K,M}/G_{Na,M}$	Diffusion	Cable	Diffusion	Cable	Diffusion	Cable
0.1	1.01	1.07	1.02	1.07	1.07	1.07
1	1.11	1.18	1.24	1.33	1.58	1.79
10	6.05	8.03	7.35	17.65	1.70	47.53
100	*	*	*	*	1.66	*

F factors at the spine head when both excitatory and K^+-mediated inhibitory synaptic inputs are located on the same spine predicted by both the electrodiffusion and the cable models.
*F factors undefined because the responses were hyperpolarizing, indicating very effective inhibition.

prediction is consistent with the finding that $GABA_B$ input to hippocampal pyramidal cells is preferentially dendritic (17), where the majority of inputs are onto spines. Another way to have effective inhibition on a spine is through conductance decreases of either Na^+ or Ca^{2+}, although this type of inhibitory mechanism has not been found in cortical neurons.

The best estimates available for the synaptic conductance changes on spines are in the range of 0.1 to 10 nS. Our simulations show that shunting inhibition of this size can at best achieve an F factor of ≈ 2. The proposal that shunting inhibition enables a dendritic tree to perform many spatially localized logical operations, such as directional selectivity in visual neurons, should be reconsidered (2).

Our simulations have shown that discrepancies between the cable model and our electrodiffusion model increase with the magnitude and duration of the synaptic conductance changes. Since the cable model is valid only when the concentration changes are small, we can derive a condition under which the cable model is self-consistent. The intracellular concentration change of the kth ionic species caused by membrane current I_k within time duration Δt is $\Delta n_k = I_k \Delta t / vzF$, where v is the effective intracellular volume, z is the valence of the ion involved, and F is the Faraday constant. (Of course, n_k will eventually stop changing with time when the membrane current is balanced by the intracellular diffusion.) The criterion for the self-consistency of the cable model is simply $|\Delta n_k|/n_{k,0} << 1$, where $n_{k,0}$ is the initial intracellular ionic concentration, or, $\Delta t << |vzFn_{k,0}/I_k|$. When the synaptic conductance G_k is small, say 0.1 nS, $I_k \approx G_k E_k$, where E_k is the reversal potential relative to the resting potential. The above condition gives $\Delta t << 10$ ms for Na^+ in a spine, assuming that the effective volume v is equal to twice the volume of the spine. Therefore, the cable model may not be valid for spines if the duration of the conductance change is longer than 10 ms even for synaptic conductance changes as small as 0.1 nS. The inclusion of ionic pumps would not alter the above conclusions for a typical Na–K pump current density of 1 $\mu A/cm^2$ (18), in which case the total pump current of the spine head is ≈ 10 fA, 3 orders of magnitude smaller than the synaptic current. Even when the pump molecules are close-packed in the membrane, the maximum possible pump current density is 100 $\mu A/cm^2$ and the total pump current of the spine head is still ≈ 10 times smaller than the synaptic current for a 0.1-nS conductance. The effect of the Na–K pump would be significant if we assume that the spine apparatus is also densely packed with pump molecules and its surface area is ≈ 10 times that of the spine.

Large compartments such as cell bodies and thick dendrites do not suffer from the concentration effects that reduce the effectiveness of inhibition in smaller structures such as spines. On the other hand, large compartments are also harder to depolarize, which is needed to increase the driving force for the inhibitory currents. This second factor may not be as important if a compartment also receives a large number of convergent excitatory synapses. Note that the more depolarized a cell, the more effective the inhibitory synapses become and the less effective the excitatory synapses. Indeed, if the depolarization is large enough to trigger an action potential, the driving forces for the inhibitory currents on the soma and dendrites reach their maximum and the driving forces for the excitatory currents reach their minimum, especially if the effects of the action potentials propagate up the dendritic tree. Thus, inhibitory synapses on the cell body and proximal dendrites could control the effects of action potentials propagating up dendritic trees and the temporal firing patterns of the neuron (W. W. Lytton and T.J.S., unpublished data).

We are grateful to Francis Crick and Christof Koch for helpful discussions. This research was supported by the Mathers Foundation, the Drown Foundation, and Office of Naval Research Grant N00014-89-J-1766.

1. Koch, C. & Poggio, T. (1983) *Proc. R. Soc. London Ser. B* **218,** 455–477.
2. Koch, C., Poggio, T. & Torre, V. (1983) *Proc. Natl. Acad. Sci. USA* **80,** 2799–2802.
3. Rall, W. (1977) in *Handbook of Physiology: The Nervous System*, ed. Kandel, E. R. (Am. Physiol. Soc., Bethesda, MD), pp. 39–97.
4. Koch, C., Poggio, T. & Torre, V. (1982) *Philos. Trans. R. Soc. London Ser. B* **298,** 227–264.
5. Higashima, M., Sawada, S. & Yamamoto, C. (1986) *Neurosci. Lett.* **68,** 221–226.
6. Brown, T., Chang, V., Ganong, A., Keenan, C. & Kelso, S. (1988) in *Long-Term Potentiation: From Biophysics to Behavior*, eds. Landfield, P. & Deadwyler, S. (Liss, New York), pp. 201–264.
7. Qian, N. & Sejnowski, T. J. (1988) in *Cellular Mechanisms of Conditioning and Behavioral Plasticity*, eds. Woody, C. W., Alkon, D. L. & McGaugh, J. L. (Plenum, New York), pp. 237–244.
8. Qian, N. & Sejnowski, T. J. (1989) *Biol. Cybern.* **62,** 1–15.
9. Griffith, W., Brown, T. & Johnston, D. (1986) *J. Neurophysiol.* **55,** 767–775.
10. Huguenard, J. & Alger, B. (1986) *J. Neurophysiol.* **56,** 1–18.
11. Hille, B. (1984) *Ionic Channels of Excitable Membranes* (Sinauer, Sunderland, MA), p. 240.
12. Beaulieu, C. & Colonnier, M. (1985) *J. Comp. Neurol.* **231,** 180–189.
13. Koch, C. & Poggio, T. (1983) *Trends Neurosci.* **3,** 80–83.
14. Miles, R. & Wong, R. (1984) *J. Physiol. (London)* **356,** 97–113.
15. Martin, K. F. (1984) in *Cerebral Cortex*, eds. Peters, A. & Jones, E. G. (Plenum, New York), Vol. 1, pp. 123–200.
16. Harris, K. M. & Stevens, J. K. (1989) *J. Neurol.* **9,** 2982–2997.
17. Janigro, D. & Schwartzkrion, P. (1988) *Brain Res.* **453,** 265–274.
18. Weer, P. D. & Rakowski, R. F. (1984) *Nature (London)* **309,** 450–452.